

## Solar Photospheric Magnetic Flux Tubes: Theory

The magnetic field in the photospheric layers of the Sun is found to occur not in a homogeneous form but in discrete concentrations of intense field. The most obvious form of magnetic flux (magnetic field strength times surface area occupied by the field) is seen in SUNSPOTS but it turns out that much smaller arrangements of magnetic field are to be found in the lanes between granules where downdraughts occur (see SOLAR PHOTOSPHERE: GRANULATION). These are the photospheric flux tubes: small-scale concentrations of intense magnetic field. The tubes have diameters of a few hundred kilometers or smaller and field strengths of 1–2 kG. Generally found in intergranular lanes, they are subject to the dynamical nature of the photospheric environment with its sound waves and flows. The tubes are isolated flux tubes in that their immediate surroundings are essentially field-free. See SOLAR PHOTOSPHERIC MAGNETIC FLUX TUBES: OBSERVATIONS.

The small-scale tubes of the photosphere may be thought of as the elemental building blocks of solar magnetism, so an understanding of intense flux tubes has implications for a wider understanding of solar and stellar magnetic phenomena. Theoretical progress in modelling small-scale flux tubes builds on the fact that in such tubes variations across the interior of a tube are less important than variations along the tube.

The elemental photospheric flux tube is taken to be a cylinder of magnetic flux embedded in a field-free environment; the photospheric flux tube is thus a region of locally high Alfvén speed. Two basic speeds prove central to an understanding of tube dynamics: the slow tube speed  $c_t$  and the kink speed  $c_k$ . These speeds are in turn defined in terms of the sound speed and Alfvén speed. For a tube of magnetic field strength  $B_0$  with plasma density  $\rho_0$  and pressure  $p_0$ , the sound speed  $c_s$  and Alfvén speed  $v_A$  of the tube are defined by

$$c_s = \left( \frac{\gamma p_0}{\rho_0} \right)^{1/2} \quad v_A = \left( \frac{B_0^2}{\mu \rho_0} \right)^{1/2} \quad (1)$$

where  $\gamma$  (generally taken to be 5/3) is the ratio of specific heats of the plasma and  $\mu$  is its magnetic permeability.

From the speeds  $c_s$  and  $v_A$  we may construct the slow magnetoacoustic speed  $c_t$  and the kink speed  $c_k$  of a tube:

$$c_t = \frac{c_s v_A}{(c_s^2 + v_A^2)^{1/2}} \quad c_k = \left( \frac{\rho_0}{\rho_0 + \rho_e} \right)^{1/2} v_A \quad (2)$$

here  $\rho_e$  denotes the plasma density of the field-free environment of the tube. The slow tube speed and the kink speed are important in coronal flux tubes too (see MAGNETOHYDRODYNAMIC WAVES).

A photospheric flux tube is typically a region of plasma density depletion: the presence of the magnetic field leads to a plasma pressure reduction inside the tube, in keeping with the requirement of transverse pressure

balance, and unless there are substantial temperature differences between the tube and its environment then this reduction in plasma pressure is accompanied by a reduction in plasma density. In other words, the magnetic field of a photospheric flux tube partially evacuates the plasma. This is in contrast to the coronal flux tube which is generally a region of plasma enhancement and reduced Alfvén speed, achieved without violation of pressure balance because the strong and pervasive magnetic field of the solar corona can easily accommodate any enhancements or reductions in the plasma pressure.

The thermal structure of a photospheric flux tube is complicated. The tube may exchange heat with its surroundings, through radiative transport and convective energy transport. Detailed numerical studies suggest that photospheric magnetic flux tubes are hotter than their surroundings in their upper layers but cooler than their surroundings in their deeper layers.

The speeds  $c_t$  and  $c_k$  of a photospheric flux tube are sub-Alfvénic, and the slow speed is also sub-sonic; whether the kink speed is sub-sonic depends on the specific parameters of the tube. A numerical illustration is of interest. In a photospheric flux tube with  $B_0 = 2$  kG and plasma density  $\rho_0 = 2.2 \times 10^{-4}$  kg m<sup>-3</sup>, the Alfvén speed is  $v_A = 12$  km s<sup>-1</sup>. Taking the sound speed  $c_s$  of the photosphere to be 8 km s<sup>-1</sup> then gives a slow speed of  $c_t = 6.7$  km s<sup>-1</sup>. For a flux tube that has depleted its plasma density to some 50% of its environment (so that  $\rho_0 = \rho_e/2$ , consistent with an environment sound speed of 9.6 km s<sup>-1</sup>), we obtain  $c_k = 6.9$  km s<sup>-1</sup>. Thus the slow speed  $c_t$  is some 56% of the Alfvén speed and the kink speed  $c_k$  is about 57% of the Alfvén speed. The precise ordering of the two speeds depends on the details of the modelling.

The speeds  $c_t$  and  $c_k$  are associated with the dynamics of flux tubes, arising in both wave phenomena and flows in tubes. The speed  $c_t$ , made up in equal measure of the sound speed and the Alfvén speed, is evidently associated with the compressibility of the tube. Any squeezing of a tube results in increases in the magnetic pressure and plasma pressure in the tube, which act to restore the undisturbed state. This is a feature shared by all elastic tubes and consequently the equivalent of the speed  $c_t$  arises in a variety of other physical situations, with the role of the Alfvén speed being played by the appropriate elastic speed of an elastic tube. For example, in the case of a blood vessel the equivalent of the speed  $v_A$  is simply the elastic speed in the membrane of the blood vessel. The speed of sound  $c_s$  in blood is much larger than the elastic speed and so the slow speed is close to the elastic speed of the blood vessel. For water in a pipe, the relative magnitudes of the two basic speeds depend on the material of the pipe. In a metal pipe, the elastic speed is much larger than the sound speed in water and so the effective slow speed is close to the sound speed in water (about 1.4 km s<sup>-1</sup>). By contrast, in a plastic pipe the orderings in the two speeds are reversed and the effective propagation speed is close to the elastic speed in plastic

(about  $10 \text{ m s}^{-1}$ ), lying far below the speed of sound in water.

The kink speed involves both the tube and its environment. The kink wave which propagates with this speed (see below) involves the magnetic tension force in the tube and the kink wave displaces both the tube and its surroundings by about equal measures, hence the combined occurrence of the densities  $\rho_0$  and  $\rho_e$ . The speed also arises in the description of magnetoacoustic surface waves on an interface between two plasmas of different properties.

An important question in the physics of photospheric flux tubes is how are they formed. A flux tube with kilogauss field strength requires strong forces to bring about its intense state, with the magnetic pressure  $B_0^2/2\mu$  being far in excess of the pressure of converging flows that granulation may provide; the tube finds equilibrium through evacuation of its interior, reducing the plasma pressure and thus allowing magnetostatic pressure balance between the flux tube and its environment to occur. It is envisaged that granulation acts to ‘shepherd’ flux tubes into the regions where downdraughts between the granules occur. The process is an example of flux expulsion (by advection), whereby the convective flows of the photosphere move magnetic field into intergranular lanes, in keeping with the frozen flux concept of ideal MAGNETOHYDRODYNAMICS. The process is not of itself sufficient to account for the observed field strengths; it brings about the ‘seedlings’ of photospheric flux tubes but other effects are needed to produce the observationally determined intense field strengths. The additional process that comes into play is driven by the super-adiabatic temperature gradient of the solar convection zone (see SOLAR INTERIOR: CONVECTION ZONE), which in field-free regions drives the convective flows (granules and supergranules; see SOLAR PHOTOSPHERE: SUPERGRANULATION) that distinguish the Sun’s convection. In flux tubes, convectively driven flows are channelled by the tubes. The fact that photospheric flux tubes reside in a plasma that is stratified by gravity means that any downdraught generated within a flux tube brings less dense plasma from the higher reaches of the stratified tube to the deeper layers within the tube, allowing the high plasma pressure of the environment to squeeze the tube further. An increase in magnetic field strength results. The process is referred to as convective collapse. It may be described in mathematical detail for a thin flux tube (see below).

A flow in a magnetic flux tube may also develop because of pressure differences between the footpoints of the tube. For example, if the footpoints of a tube are rooted in regions that are magnetically distinct from one another, such as one footpoint in a sunspot and the other in a field-free region, then plasma pressure differences arise and a flow may be driven in the tube. Such motions of the plasma within the tube are called siphon flows.

### Waves in photospheric flux tubes

To give a detailed description of the magnetohydrodynamic waves that an isolated photospheric flux tube supports we consider the equations of ideal MHD. Consider an equilibrium magnetic field  $B_0 = B_0(r)\hat{z}$  aligned with the  $z$ -axis of a cylindrical polar coordinate system  $(r, \theta, z)$ . To begin with we will ignore the effects of gravity. Then the equilibrium plasma pressure  $p_0(r)$  of a radially structured magnetic atmosphere is such as to maintain total pressure balance: the sum of the plasma pressure  $p_0(r)$  and the magnetic pressure  $B_0^2(r)/2\mu$  is a constant. Where the field is strong, as in the center of a flux tube, the plasma pressure is correspondingly reduced.

Small-amplitude motions  $v = (v_r, v_\theta, v_z)$  about a structured equilibrium state satisfy the coupled wave equations

$$\rho_0(r) \left( \frac{\partial^2}{\partial t^2} - v_A^2(r) \frac{\partial^2}{\partial z^2} \right) v_r + \frac{\partial^2 p_T}{\partial r \partial t} = 0 \quad (3)$$

$$\rho_0(r) \left( \frac{\partial^2}{\partial t^2} - v_A^2(r) \frac{\partial^2}{\partial z^2} \right) v_\theta + \frac{1}{r} \frac{\partial^2 p_T}{\partial \theta \partial t} = 0 \quad (4)$$

$$\left( \frac{\partial^2}{\partial t^2} - c_t^2(r) \frac{\partial^2}{\partial z^2} \right) v_z = - \frac{c_s^2(r)}{c_s^2(r) + v_A^2(r)} \frac{1}{\rho_0(r)} \frac{\partial^2 p_T}{\partial z \partial t} \quad (5)$$

with the evolution of  $p_T(r, \theta, z)$  described by

$$\frac{\partial p_T}{\partial t} = \rho_0(r) v_A^2(r) \frac{\partial v_z}{\partial z} - \rho_0(r) [c_s^2(r) + v_A^2(r)] \text{div } v. \quad (6)$$

Here  $c_t(r)$ ,  $c_s(r)$  and  $v_A(r)$  denote the slow speed, sound speed and Alfvén speed within the radially structured plasma, of density  $\rho_0(r)$ . Equations (3)–(5) come from the components of the momentum equation in which the magnetic force has been expressed in terms of the perturbation in total pressure  $p_T$ , defined as the sum of the perturbation  $p$  in the dynamical plasma pressure and the magnetic pressure perturbation  $B_0(r)B_z/\mu$ , with  $B_z$  being the component of the perturbed magnetic field in the direction of the applied magnetic field  $B_0$ . Equation (6) results from a combination of the isentropic (adiabatic) equation and the induction equation of ideal MHD.

One solution of the above equations is the torsional Alfvén wave, which propagates motions  $v_\theta$ , independent of  $\theta$ , according to the wave equation

$$\frac{\partial^2 v_\theta}{\partial t^2} = v_A^2(r) \frac{\partial^2 v_\theta}{\partial z^2}. \quad (7)$$

Torsional oscillations, which have  $v_r = 0$ ,  $v_z = 0$  and  $p_T = 0$ , have a radial dependence determined by the manner in which the oscillations are generated. The oscillations exhibit phase mixing by which radial gradients of the motion grow rapidly in regions where the Alfvén speed  $v_A(r)$  varies sharply in  $r$ .

In addition to torsional Alfvén waves there are motions that are compressive, with  $p \neq 0$  and  $p_T \neq 0$ . We examine the elemental magnetic flux tube that models photospheric conditions, taking the applied magnetic field

$B_0(r)\hat{z}$  to be confined within a cylindrical tube of radius  $a$ . The plasma pressure and density within the tube are  $p_0$  and  $\rho_0$ ; the corresponding plasma pressure and density in the tube's field-free environment are  $p_e$  and  $\rho_e$ . The tube is in magnetostatic pressure balance with its surroundings:  $p_e = p_0 + B_0^2/2\mu$ . With  $c_s$  and  $v_A$  now denoting the sound speed and Alfvén speed within the tube and  $c_e$  the sound speed in the tube's environment, pressure balance combined with the ideal gas law then shows that the plasma density  $\rho_0$  within the tube is related to the density  $\rho_e$  in the tube's environment through

$$\frac{\rho_0}{\rho_e} = \frac{c_e^2}{c_s^2 + \frac{1}{2}\gamma v_A^2}. \quad (8)$$

Thus, for sound speeds  $c_s$  and  $c_e$  that are roughly comparable, a photospheric flux tube is a region of density depletion (i.e.  $\rho_0 < \rho_e$ ).

Now the media inside and outside the elemental flux tube are uniform, and this affords a considerable simplification. In a uniform medium, the wave equations (3)–(6) may be combined to yield an equation for  $p_T$ . Writing

$$p_T(r, \theta, z, t) = p_T(r) \exp i(\omega t + n\theta - k_z z)$$

provides a Fourier description of the motions, of frequency  $\omega$ , longitudinal wavenumber  $k_z$  and azimuthal number  $n$ . The integer  $n (= 0, 1, 2, \dots)$  describes the geometrical form of the perturbations. The case  $n = 0$  gives the sausage wave and corresponds to symmetric squeezings and rarefactions of the tube; these are compressional ( $p_T \neq 0$ ) oscillations. The case  $n = 1$  describes the kink wave of the tube; in such waves the motion of the tube resembles a wriggling snake, with the whole tube being displaced without changing its cross-sectional shape. Finally, there are also waves with  $n \geq 2$ ; these are the fluting waves.

For a uniform tube,  $p_T$  satisfies

$$r^2 \frac{d^2 p_T}{dr^2} + r \frac{dp_T}{dr} - (m_0^2 r^2 + n^2) p_T = 0 \quad (9)$$

where

$$m_0^2 = \frac{(k_z^2 c_s^2 - \omega^2)(k_z^2 v_A^2 - \omega^2)}{(c_s^2 + v_A^2)(k_z^2 c_e^2 - \omega^2)}.$$

This is a form of Bessel's equation with solution  $p_T = I_n(m_0 r)$  inside ( $r < a$ ) the tube;  $I_n$  is a modified Bessel function. Similarly, in the field-free environment ( $r > a$ ) of the flux tube, where the sound speed is  $c_e$ , a solution  $p_T$  proportional to the modified Bessel function  $K_n(m_e r)$  arises, where

$$m_e^2 = k_z^2 - \frac{\omega^2}{c_e^2}.$$

It is usual to examine modes for which  $m_e^2$  is positive, corresponding to selecting waves that are confined to near the tube. Then, matching  $p_T$  and  $v_r$  across  $r = a$  results in

$$\frac{1}{\rho_0(k_z^2 v_A^2 - \omega^2)} m_0 \frac{I_n'(m_0 a)}{I_n(m_0 a)} + \frac{1}{\rho_e \omega^2} m_e \frac{K_n'(m_e a)}{K_n(m_e a)} = 0 \quad (10)$$

where a prime ( $'$ ) denotes the derivative of a modified Bessel function (e.g.  $I_n'(m_0 a) \equiv dI_n(x)/dx$  evaluated at  $x = m_0 a$ , etc). This is the dispersion relation for tube waves in an isolated magnetic flux tube, requiring that  $m_e > 0$ ; surface waves arise whenever  $m_0^2 > 0$ , and body waves occur if  $m_0^2 < 0$ . It is evident that tube waves are dispersive, their phase speed  $c (\equiv \omega/k_z)$  depending on the wavenumber (in the combination  $k_z a$ ).

Solution of the dispersion relation (10), for conditions appropriate for an isolated photospheric flux tube, show that there are slow body waves (both sausage and kink) with phase speeds  $c$  that lie between  $c_t$  and  $c_s$  and slow surface waves which have phase speeds that are less than  $c_t$ . Also, there is a surface wave with a phase speed close to the kink speed  $c_k$  and another surface wave with phase speed near  $c_e$ . Fluting modes also have speeds close to  $c_k$ .

There is particular interest in waves that are much longer than a tube diameter, corresponding to  $k_z a \ll 1$ . This is the thin flux tube limit, of special interest for photospheric flux tubes. Since generally  $\omega \sim k_z v_A$ , the condition  $k_z a \ll 1$  corresponds to requiring that periods  $\tau (\equiv 2\pi/\omega)$  are such that  $\tau \gg 2\pi a/v_A$ , giving  $\tau \gg 50$  s for a tube of radius  $a = 100$  km. P-modes, for example, have periods around 300 s, roughly meeting this criterion. With  $k_z a \ll 1$ , the slow surface wave has phase speed close to  $c_t$ .

Dispersion relations such as equation (10) are important in the development of a nonlinear wave theory for a tube. Indeed, it has been shown that slow (sausage) surface waves have motions  $v(z, t)$  along a thin tube which satisfy the nonlinear integrodifferential equation

$$\frac{\partial v}{\partial t} + c_t \frac{\partial v}{\partial z} + \beta_0 v \frac{\partial v}{\partial z} + \alpha_0 \frac{\partial^3}{\partial z^3} \int_{-\infty}^{\infty} \frac{v(s, t) ds}{[\lambda^2 a^2 + (z-s)^2]^{1/2}} = 0. \quad (11)$$

The constants  $\alpha_0$ ,  $\beta_0$  and  $\lambda$  depend on the various parameters of the tube.

Equation (11) is sometimes referred to as the Leibovich–Roberts equation. An explicit form of its solution is not known although it is amenable to numerical solution. It is of particular interest because it is associated with soliton behavior. Solitons are nonlinear waves with specific interaction properties that make them worthy of special study. For the related problem of a magnetic slab—the Cartesian equivalent of a flux tube—the equation describing the weakly nonlinear slow surface wave is the Benjamin–Ono equation, i.e.

$$\frac{\partial v}{\partial t} + c_t \frac{\partial v}{\partial z} + \beta_0 v \frac{\partial v}{\partial z} + \alpha_1 \frac{\partial^2}{\partial z^2} \int_{-\infty}^{\infty} \frac{v(s, t)}{s-z} ds = 0 \quad (12)$$

for constant  $\alpha_1$ . The Benjamin–Ono equation has been studied extensively and its soliton solution is known explicitly. Equations (11) and (12) may be derived using thin flux tube theory (see below) or from the full equations of ideal MHD, assuming that motions are weakly nonlinear and weakly dispersive.

### Thin flux tube theory

The restriction to thin tubes, in the sense that waves are much longer than a tube radius (so that  $k_z a \ll 1$ ), leads to a considerable simplification in the description of the dynamics of photospheric flux tubes, so much so that it becomes possible to include a number of other effects ignored in the discussion of an elemental magnetic flux tube. Of particular importance is the influence of stratification brought about by gravity. The pressure scale height in the photosphere is comparable with a tube radius so the effects of gravity are particularly significant in the photospheric layers of a tube. Other effects, such as radiative transport, may also in principle be included in thin flux tube theory.

To describe motions in a thin tube in the presence of gravity the so-called thin flux tube equations are used. These equations have been used extensively for both analytical and numerical investigations of flux tube dynamics. The sausage and kink modes are treated separately. The thin tube equations for the *sausage mode* (in ideal MHD) are

$$\frac{\partial}{\partial t} \rho A + \frac{\partial}{\partial z} \rho v A = 0 \quad (13)$$

$$\frac{\partial v}{\partial t} + v \frac{\partial v}{\partial z} = -\frac{1}{\rho} \frac{\partial p}{\partial z} - g \quad (14)$$

$$\frac{\partial p}{\partial t} + v \frac{\partial p}{\partial z} = \frac{\gamma p}{\rho} \left( \frac{\partial \rho}{\partial t} + v \frac{\partial \rho}{\partial z} \right) \quad (15)$$

$$B A = \text{constant} \quad (16)$$

$$p + \frac{B^2}{2\mu} = p_e. \quad (17)$$

In these equations,  $B(z, t)$  is the field strength of a thin tube with cross-sectional area  $A(z, t)$ , and  $v(z, t)$  is the longitudinal flow speed within the tube, where the plasma pressure and density are  $p(z, t)$  and  $\rho(z, t)$ . The gravitational acceleration is  $g (= 274 \text{ m s}^{-2})$ , acting in the negative  $z$ -direction. The external gas pressure  $p_e(z, t)$  is calculated on the boundary of the tube and may vary in response to motions in the tube or its environment; pressure balance across the tube is maintained at all times (as expressed by equation (17)).

In equilibrium ( $v = 0, \partial/\partial t = 0$ ) the thin tube equations for a magnetic flux tube in temperature balance with its surroundings (so that  $c_s = c_e$ ) yield

$$\begin{aligned} p_0(z) &= p_0(0) e^{-N} & \rho_0(z) &= \rho_0(0) \frac{\Lambda_0(0)}{\Lambda_0(z)} e^{-N} \\ A_0(z) &= A_0(0) e^{N/2} & B_0(z) &= B_0(0) e^{-N/2} \end{aligned} \quad (18)$$

where

$$N(z) = \int_0^z \frac{dz}{\Lambda_0(z)}$$

is the integrated pressure scale height;  $\Lambda_0(z) (\equiv p_0(z) g \rho_0(z))$  is the pressure scale height inside the tube. See figure 1.

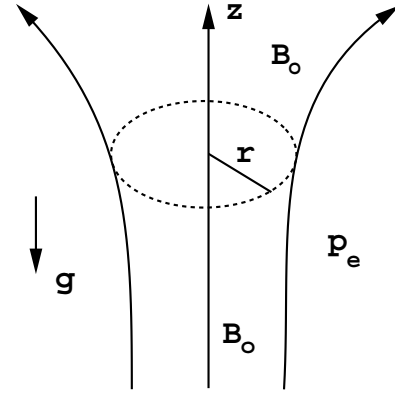


**Figure 1.** Equilibrium state of a thin magnetic flux tube in a stratified plasma. The tube is confined by the external plasma pressure  $p_e$  in the field-free environment of the tube. The region within the tube is generally of lower plasma density than the environment.

The linear form of the thin tube equations is readily found for the equilibrium (18). Ignoring contributions from variations in  $p_e$ , longitudinal motions are found to satisfy the Klein–Gordon equation

$$\frac{\partial^2 Q}{\partial t^2} - c_t^2(z) \frac{\partial^2 Q}{\partial z^2} + \Omega_s^2(z) Q = 0 \quad (19)$$

where  $Q(z, t)$  is related to the flow  $v(z, t)$  and  $\Omega_s^2(z)$  depends on the details of the equilibrium state.

In an isothermal atmosphere,  $\Lambda_0$ ,  $c_t$  and  $\Omega_s^2$  are all constants, with

$$\Omega_s^2 = \frac{c_t^2}{4\Lambda_0^2} \left[ \left( \frac{9}{4} - \frac{2}{\gamma} \right) + \frac{4c_s^2}{\gamma v_A^2} \left( 1 - \frac{1}{\gamma} \right) \right]. \quad (20)$$

The Klein–Gordon equation (19) then yields the dispersion relation

$$\omega^2 = k_z^2 c_t^2 + \Omega_s^2 \quad (21)$$

which shows that  $\Omega_s$  is a cutoff frequency (for sausage waves in a thin tube).  $\Omega_s^2$  may be viewed as made up of two contributions, the first (corresponding to the first term on the right-hand side of equation (20)) arising from the geometrical shape of the undisturbed tube and the second (corresponding to the second term on the right of equation (20)) being determined by the tube's elasticity. A rigid tube with exponential cross-sectional area (determined according to the equilibrium (18) with  $\Lambda_0$  constant) has cutoff frequency  $(9/4 - 2/\gamma)^{1/2} c_s/2\Lambda_0$ , whereas a straight and vertical rigid tube has cutoff frequency  $c_s/2\Lambda_0$ . In general the cutoff frequency for the sausage mode in a tube is less than the cutoff frequency of a rigid tube.

The Klein–Gordon equation also describes the kink mode in a thin tube. Thin tube equations for the kink mode may be used to describe the transverse displacements  $\xi(z, t)$  of a vertical tube, leading to the wave equation

$$\frac{\partial^2 \xi}{\partial t^2} = c_k^2(z) \frac{\partial^2 \xi}{\partial z^2} + g \left( \frac{\rho_0 - \rho_e}{\rho_0 + \rho_e} \right) \frac{\partial \xi}{\partial z}. \quad (22)$$

Equation (22) may be cast into an equation of the Klein–Gordon form, just as for the sausage mode. For an isothermal medium, the dispersion relation for the kink mode is

$$\omega^2 = k_z^2 c_k^2 + \Omega_K^2 \quad (23)$$

where the cutoff frequency for the kink mode is

$$\Omega_K = \frac{c_k}{4\Lambda_0}. \quad (24)$$

The forms (19)–(24) allow a direct comparison between sausage and kink modes. For example, with again  $v_A = 12 \text{ km s}^{-1}$ ,  $c_s = 8 \text{ km s}^{-1}$  and  $\Lambda_0 = 140 \text{ km}$ , sausage and kink modes both grow in amplitude by a factor of  $e$  in propagating a distance of  $560 \text{ km}$  (four scale heights). The sausage wave, propagating with a speed  $c_t = 6.7 \text{ km s}^{-1}$ , has a cyclic cutoff frequency,  $\Omega_s/2\pi$ , of  $4.2 \text{ mHz}$  (period  $240 \text{ s}$ ). The kink wave has a speed of  $c_k = 6.9 \text{ km s}^{-1}$ , close to the sausage mode's, but its cutoff frequency at  $2 \text{ mHz}$  (period  $500 \text{ s}$ ) is very different. The sausage mode's behavior is similar to that of a vertically propagating sound wave, which has a propagation speed of  $8 \text{ km s}^{-1}$  and cutoff frequency of  $4.5 \text{ mHz}$  (period  $220 \text{ s}$ ), although it  $e$ -folds in just  $280 \text{ km}$  (two scale heights); consequently, sound waves are expected to form shocks lower in the atmosphere than tube waves. The fact that the cutoff frequency of the kink mode is considerably smaller than the cutoff frequency of the sausage wave or a sound wave suggests that kink waves may survive to higher levels in the solar atmosphere than sausage waves or sound waves.

The dispersion relations (21) and (23) imply that an impulsively generated wave (sausage or kink) results in a wavefront which propagates with the speed  $c_t$  or  $c_k$ , the wavefront supporting an oscillating wake which rises and falls with the frequency  $\Omega_s$  or  $\Omega_K$ .

### Convective collapse

Convective collapse, the process by which a photospheric flux tube may be formed with kilogauss field strengths, may be demonstrated from the thin flux tube equations for the sausage mode. The differential equation satisfied by the longitudinal flow, Fourier analyzed by writing  $v(z, t) = u(z) \exp(i\omega t)$ , is

$$\frac{B_0}{\rho_0} \frac{d}{dz} \left( \frac{\rho_0 c_t^2}{B_0} \frac{du}{dz} \right) + \left[ \omega^2 - \omega_g^2 \left( \frac{c_t^2}{v_A^2} + \frac{\gamma c_t^2}{2c_s^2} \right) \right] u = 0 \quad (25)$$

where

$$\omega_g^2 = \frac{g}{\Lambda_0} \left( \Lambda'_0 + \frac{\gamma - 1}{\gamma} \right)$$

is the square of the Brunt–Väisälä (or buoyancy) frequency of a plasma element in a stratified atmosphere. In the atmosphere of a flux tube embedded within the solar convection zone,  $\omega_g^2$  is negative and this drives an instability within the tube. The magnetic field may quench the instability if it is sufficiently strong. This is readily illustrated by an approximate solution of equation (25).

With the illustrative boundary conditions that  $u = 0$  at levels  $z = 0$  and  $z = -d$ , we obtain the approximate solution

$$u(z) = u_0 \exp\left(\frac{z}{4\Lambda_0}\right) \sin\left(\frac{\pi z}{d}\right) \quad (26)$$

with

$$\omega^2 = c_t^2 \left[ \frac{\pi^2}{d^2} + \frac{1}{16\Lambda_0^2} + \left( \frac{1}{v_A^2} + \frac{\gamma}{2c_s^2} \right) \omega_g^2 \right].$$

Hence, if  $\omega_g^2 < 0$  then a mode with  $\omega^2 < 0$  may arise, corresponding to an instability. The instability amounts to a flow of plasma within the stratified tube; a downdraught brings the more tenuous plasma in the higher levels of the tube to layers deeper within the tube, allowing the external plasma pressure to squeeze the tube. A stronger field results. This is convective collapse. The process is halted when the field strength  $B_0$  is sufficiently large to resist the compression of the tube, and so quench the instability (reducing  $\omega^2$  to zero). A flux tube with only moderate field strength finds itself subject to the instability until it has strengthened itself, through convective collapse, to a state where it may resist the process. Consequently, intense and isolated magnetic flux tubes are the expected norm in any medium such as the solar photosphere where convective effects operate in the presence of magnetic field.

A determination of the field strength necessary to quench the instability depends on the precise details of the modelling. Studies of the process under conditions appropriate for the solar convection zone show that kilogauss field strengths are required before the collapse is halted. However, what precisely is the ensuing state of a collapsed flux tube remains uncertain, mainly as a result of the need to take into account a number of detailed and complicated effects ignored in the above treatment. In particular, it is necessary to include the effects of RADIATIVE TRANSFER, nonlinearity and a more realistic choice of flow boundary conditions.

### Numerical simulations

Numerical simulations allow the inclusion of a variety of effects that complicate the description of the basic modes of behavior of photospheric flux tubes, and this promotes a more direct comparison with solar observations. By following the motion of a parcel of magnetized fluid (using a so-called Lagrangian approach), it proves possible, for example, to explore the linear and nonlinear sausage and kink modes in a vertical tube or to simulate the convective collapse process. These problems are usually addressed through numerical solution of thin flux tube equations, allowing for the important effects of stratification. Broadly, analytic theory for an ideal plasma has provided valuable insights for the more complex modelling of flux tubes under conditions representative of the solar photosphere. Thin flux tube theory for the kink mode has also been applied to modelling the behaviour of a nonvertical flux tube, addressing in particular the important question of

how magnetic field stored below the convection zone is transported to the solar surface.

An important question still under active consideration is how to incorporate the environment's back-reaction on a moving flux tube. The effect has been explored for the sausage mode and leads to the formation of solitons; the influence of stratification on flux tube solitons has not so far been explored. The back-reaction of the environment on the kink mode is somewhat uncertain, with several alternative possibilities suggested in the literature.

The behaviour of shocks excited within tubes and also the formation of shocks and downflows as a result of the convective collapse of a tube have been modelled in two-dimensional simulations. Numerical simulations have also permitted realistic estimates of the energy flux carried by the various waves, allowing applications to the Sun and stellar atmospheres more generally to be explored.

#### *Bibliography*

- Hollweg J V 1990 MHD waves on solar magnetic flux tubes *Physics of Magnetic Flux Ropes (Geophys. Monogr. 58)* ed C T Russell, E R Priest and L C Lee (Washington, DC: AGU) p 23
- Parker E N 1979 *Cosmical Magnetic Fields* (Oxford: Oxford University Press) pp 841
- Roberts B 1992 Magnetohydrodynamic waves in structured magnetic fields *Sunspots: Theory and Observations* ed J H Thomas and N O Weiss (Dordrecht: Kluwer) p 303
- Roberts B and Ulmschneider P 1997 Dynamics of flux tubes in the solar atmosphere: theory *Solar and Heliospheric Plasma Physics* ed G M Simnett, C E Alissandrakis and L Vlahos (Berlin: Springer) p 75
- Ryutova M P 1990 Waves and oscillations in magnetic flux tubes *Solar Photosphere: Structure, Convection, and Magnetic Fields (IAU Symp. 138)* ed J O Stenflo (Dordrecht: Reidel) p 229
- Schüssler M 1990 Theoretical aspects of small-scale photospheric magnetic fields *Solar Photosphere: Structure, Convection, and Magnetic Fields (IAU Symp. 138)* ed J O Stenflo (Dordrecht: Reidel) p 161
- Spruit H C 1981 Magnetic flux tubes *The Sun as a Star (NASA SP-450)* ed S Jordan (Washington, DC: NASA) p 385
- Spruit H C and Roberts B 1983 Magnetic flux tubes on the Sun *Nature* **304** 401
- Spruit H C, Schüssler M and Solanki S K 1991 Filigree and flux tube physics *Solar Interior and Atmosphere* ed A N Cox, W C Livingston and M S Matthews (Tucson, AZ: University of Arizona Press) p 890

*B Roberts*